Scientific paper

Antityrosinase and Antimelanogenic Effects of Structurally Modified Kojic Acid Derivatives with Piperidine Side Chains

Gülşah Karakaya¹, Tugba Adak², Sami Hamdoun¹, Aslı Türe³, Ayşe Ercan⁴ and Mutlu Dilsiz Aytemir^{2*}

¹ İzmir Katip Çelebi University, Faculty of Pharmacy, Department of Pharmaceutical Chemistry, İzmir, Türkiye

³ Marmara University, Faculty of Pharmacy, Department of Pharmaceutical Chemistry, İstanbul, Türkiye

⁴ Hacettepe University, Faculty of Pharmacy, Department of Biochemistry, Ankara, Türkiye

* Corresponding author: E-mail: mutlud@hacettepe.edu.tr

Received: 05-11-2025

Abstract

In this study, eight QSAR models were constructed to develop novel compounds as tyrosinase inhibitors. The decision tables, Bagging, and Random Committee methods showed the best predictive abilities ($q^2 \ge 0.5$) among the models. Based on these models, twelve new kojic acid derivatives were synthesized. Tyrosinase inhibition was determined using a spectrophotometric method with L-DOPA as the substrate. Molecular docking studies were conducted to provide insights into the tyrosinase-inhibiting mechanisms of the compounds. Cytotoxic effects on the B16F10 melanoma cell line were investigated using the SRB assay. A melanogenesis assay was also performed to detect the inhibition of melanin production. Compounds **41, 4j,** and **4b** exhibited better tyrosinase inhibitory effects than the positive control, kojic acid (218.8 μ M), with IC₅₀ values of 138.1, 159.0, and 208.9 μ M, respectively. Compound **4j** showed the best anti-melanogenesis effect among the compounds tested. These findings demonstrate the potential of the compounds developed as novel tyrosinase inhibitors for clinical and cosmetic applications.

Keywords: CADD; tyrosinase; melanoma; QSAR; molecular docking

1. Introduction

Melanin pigment gives color to the skin and can be found in various living organisms, such as animals, plants, fungi, and bacteria. Its primary function is to protect the skin from harmful radiation such as UV light, free radicals, environmental pollutants, toxic drugs, and chemicals. However, excessive production or uneven distribution of melanin can lead to hyperpigmentation disorders, including malignant melanoma, melasma, postinflammatory melanoderma, freckles, lentigo, acne scars, and age spots. Recent studies have also shown that melanin plays a crucial role in the treatment of Parkinson's disease and other neurodegenerative disorders.²⁻⁴ In the agricultural industry, enzymatic darkening caused by excessive melanin production leads to the disposal of loads of fruits and vegetables.⁵ Additionally, skin-whitening products that inhibit melanin production have great economic value in the cosmetics industry.⁶ Thus, there is a high demand for melanogenesis inhibitors.

Tyrosinase (EC 1.14.18.1) is a copper-containing monooxygenase enzyme in the melanogenesis pathway, and responsible for the formation of the pigment melanin.^{7–9} Agents that prevent melanogenesis by inhibiting tyrosinase gene expression or protein degradation are limited by their off-target effects, such as irritation as direct tyrosinase inhibitors reduce melanogenesis without damaging the cells.³ Tyrosinase is thus the most often used target for inhibiting melanogenesis.

Kojic acid (5-hydroxy-2-(hydroxymethyl)-4*H*-pyran-4-one), a tyrosinase inhibitor that can be generated from secondary fungal metabolites (such as *Aspergillus spp*. and *Penicillium ssp.*) prevents enzymatic browning on many organisms including human, animals, and plants.^{6,7,10} By modifying the hydroxypyranone ring, researchers have synthesized a range of derivatives that show promising re-

² Hacettepe University, Faculty of Pharmacy, Department of Pharmaceutical Chemistry, Ankara, Türkiye

sults as tyrosinase inhibitors. ^{10–14} However, only a few of them have demonstrated acceptable potency and safety, making them suitable for practical use in the industry. So, new developments in this area are still needed.

Computer-aided drug design (CADD) has been a great asset to drug development and discovery. It is used extensively to design new drugs through various approaches, including structure-based drug design, such as molecular docking, and ligand-based drug design, such as quantitative structure-activity relationship (QSAR). Machine learning programs include algorithms that have been implemented in several areas of pharmaceutical research, including drug design, target identification and validation, and the prediction of pharmacokinetic parameters and toxicity. The use of QSAR studies employing machine learning considerably increases the likelihood of identifying valuable drug candidates, thereby reducing drug discovery time and costs.

In our laboratory, Mannich bases synthesized from kojic acid have been found to possess a broad range of biological activities including antibacterial, antifungal, antiviral, anticonvulsant, and anti-tyrosinase properties. 19-24 As secondary amine groups substituted phenyl/benzyl piperazine, piperidine or pyridines were used. These compounds exhibited potent bioactivities while being not toxic to healthy cells. As it is well known, piperidine is an important synthetic medicinal block for drugs design and is used in a wide range of pharmaceuticals including anticancer agents.²⁵ So herein, based on our findings, we developed QSAR predictive models to create new kojic acid derivatives as tyrosinase inhibitors using several machine learning algorithms. Through our previous methods and in line with the current literature data supporting this, we introduced piperidine derivatives to the 6th position of four different Mannich base groups. Compounds with the structure of 2-(4-substituted piperazine-1-yl)methyl-3-hydroxy-6-(piperidine/3-methyl piperidine/4-methyl piperidine)methyl-4H-pyran-4-one were synthesized. The structures were elucidated using IR, ¹H NMR, ¹³C NMR, mass spectroscopy, and elemental analysis. The inhibition of tyrosinase was assessed through a spectrophotometric approach utilizing L-3,4-dihydroxyphenylalanine (L-DO-PA) as the substrate. Molecular docking studies were conducted to gain insight into the mechanism of inhibition. Cytotoxicity was evaluated within B16F10 mouse melanoma cell lines via the SRB assay, while melanogenesis was analyzed to detect any inhibition of melanin production.

2. Materials and Methods

2. 1. Chemistry

All the chemicals used for the synthesis of the compounds were supplied by Merck (Darmstadt, Germany) and Aldrich Chemical Co. (Steinheim, Germany). Melting points were determined by a Thomas Hoover Capillary

Melting Point Apparatus (Philadelphia, PA, USA) and presented as uncorrected. IR spectra were recorded on a Perkin Elmer FT-IR 420 System, Spectrum BX spectrometer. ¹H and ¹³C NMR spectra were obtained with a Varian Mercury 400 MHz spectrophotometer in deutorochloroform (CDCl₃) and dimethylsulphoxide (DMSO-d₆). Tetramethylsilane (TMS) was used as an internal standard (chemical shift in δ , ppm). Mass analysis was carried out with a Micromass ZQ LCMS with Masslynx Software Version 4.1 by using the electrospray ionization (ESI+) method and HPLC with Waters Alliance by using C18 columns. Elementary analyses were performed with a Leco CHNS-932 analyzer (Leco, St. Joseph, MI, USA) in the Central Laboratory of Ankara University, Faculty of Pharmacy. The purity of the compounds was assessed by thin layer chromatography (TLC) on Kieselgel 60 F254 (Merck, Darmstadt, Germany) chromatoplates.

Synthesis of 3-hydroxy-6-chloromethyl-2-substituted- 4*H***-pyran-4-one derivatives (Mannich bases):** The first step of the synthesis pathway was obtaining the chlorokojic acid via the chlorination of kojic acid by using thionyl chloride. Phenyl piperazine derivatives, as amines and 37% formaldehyde solution, were added to MeOH. Chlorokojic acid was added to the mixture and stirred for 20 min. The solid product, as Mannich bases, was collected by filtration and washed with cold MeOH.

Synthesis of 2-((4-(substituted phenyl)piperazine-1-yl) methyl)-3-hydroxy-6-substituted piperidinyl-4*H*-pyran-4-one derivatives

Piperidine and its derivatives were dissolved in dimethyl-formamide (DMF). An appropriate Mannich base and K_2CO_3 were added to the solution, respectively. The reaction mixture was stirred for 24–36 h. The progress of the reaction was followed by TLC. After the completion of the reaction, the mixture was poured into iced water and extracted using dichloromethane. The organic phase was evaporated to dryness which were further purified by recrystallization in ethyl acetate.

2-((4-Phenylpiperazine-1-yl)methyl)-3-hydroxy-6-(piperidine-1-ylmethyl)-4*H*-pyran-4-one (4a): $C_{22}H_{29}N_3O_3$. M.W.: 383.484 g/mol; Yield: 49%; mp: 167–169 °C; %CHN Found (Calculated): C 68.63 (68.90), H 7.57 (7.62), N 10.88 (10.96); IR υ (cm⁻¹): 1620 (C=O, st), 1503, 1455 (C=C, st), 2935 (C-H, st, aliphatic), 1597 (C-C (in-ring), st), 1239, 1200 (C-N, st) 1010 (C-O, st); ¹H NMR (CDCl₃, 400 MHz) δ ppm: 1.44 (2H; m; piperidine- H^4), 1.60 (4H; m; piperidine- $H^{3,5}$), 2.46 (4H; t; J = 4.2; piperidine- $H^{2,6}$), 2.77 (4H; t; J = 5.2; piperazine- $H^{2,6}$), 3.22 (4H; t; J = 5.2; piperazine- $H^{3,5}$), 3.38 (2H; s; pyran-CH₂-piperidine), 3.74 (2H; s; pyran-CH₂-piperazine), 6.50 (1H; s; pyran- H^5), 6.86 (1H; t; J = 7.2; Ar- H^4), 6.91 (2H; d; J = 7.2; Ar- $H^{2,6}$), 7.26 (2H; m; Ar- $H^{3,5}$); ¹³C NMR (CDCl₃, 100 MHz) δ ppm: 23.89–25.87 (piperidine- $C^{3,4,5}$), 49.11–52.90 (pipera-

zine- $C^{2,3,5,6}$), 54.56 (piperidine- $C^{2,6}$), 54.99 (piperazine-C), 60.23 (piperidine-C), 111.36 (pyran- C^5), 116.22, 119.97, 129.13 (benzene- $C^{2,3,4,5,6}$), 143.86 (pyran- C^2), 145.36 (pyran- C^3), 151.08 (benzene- C^1), 165.80 (pyran- C^6), 173.96 (pyran- C^4); ESI⁺-MS (m/z): 163(100%), 384(M⁺+H).

2-((4-(4-Fluorophenyl)piperazine-1-yl)methyl)-3-hydroxy-6-(piperidine-1-ylmethyl) -4H-pyran-4-one (4b): C₂₂H₂₈FN₃O₃. M.W.: 401.474 g/mol; Yield: 43%; mp: 160-162 °C; %CHN Found (Calculated): C 65.40 (65.82), H 7.09 (7.03), N 10.38 (10.47); IR ν (cm⁻¹): 1618 (C=O, st), 1509, 1455 (C=C, st), 2938 (C-H, st, aliphatic), 1598 (C-C (in-ring), st), 1238, 1198 (C-N, st) 1010 (C-O, st); ¹H NMR (CDCl₃, 400 MHz) δ ppm: 1.43 (2H; m; piperidine- H^4), 1.58 (4H; m; piperidine- $H^{3,5}$), 2.45 (4H; t; J = 4.2; piperidine- $H^{2,6}$), 2.75 (4H; t; J = 5.2; piperazine- $H^{2,6}$), 3.13 (4H; t; J = 5.2; piperazine- $H^{3,5}$), 3.36 (2H; s; piperidine-CH₂-pyran), 3.72 (2H; s; pyran-CH₂-piperazine), 6.48 (1H; s; pyran- H^5), 6.83 (H; dd; $J_1 = 2.4$; $J_2 = 7.2$, Ar- H^2), 6.85 (H; dd; $J_1 = 2.4$; $J_2 = 6.8$, $Ar-H^6$), 6.94 (2H; m; $Ar-H^{3,5}$); ¹³C NMR (CDCl₃, 100 MHz) δ ppm: 23.90, 25.88 (piperidine- $C^{3,4,5}$), 50.10, 52.87 (piperazine- $C^{2,3,5,6}$), 54.57 (piperidine-C^{2,6}), 54.86 (piperazine-C), 60.28 (piperidine-C), 111.27 (pyran- C^5), 115.53 (d, J = 20, 4-florobenzen- $C^{3,5}$), 117.97 (\bar{d} , J = 10, 4-fluorobenzene- $C^{2,6}$), 143.83 (pyran- C^2), 145.36 (pyran- C^3), 147.74 (d, J = 1, 4-florobenzen- C^1), 157.27 (d, J = 250, 4-fluorobenzene- C^4), 165.92 (pyran- C^6), 173.96 (pyran- C^4); ESI-MS (m/z): 181 (100%), 402 (M^++H) .

2-((4-(4-Chlorophenyl)piperazine-1-yl)methyl)-3-hydroxy-6-(piperidine-1-ylmethyl)-4H-pyran-4-one (4c): C₂₂H₂₈ClN₃O₃. M.W.: 417.929 g/mol; Yield: 19%; mp: 154–155°C; %CHN Found (Calculated): C 62.78 (63.22), H 6.72 (6.75), N 9.98 (10.05); IR v (cm⁻¹): 1618 (C=O, st), 1495, 1454 (C=C, st), 2936 (C-H, st, aliphatic), 1597 (C-C (in-ring), st), 1236, 1199 (C-N, st) 1010 (C-O, st); ¹H NMR (CDCl₃, 400 MHz) δ ppm: 1.43 (2H; m; piperidine- H^4), 1.58 (4H; m; piperidine- $H^{3,5}$), 2.45 (4H; t; J = 5.2; piperidine- $H^{2,6}$), 2.74 (4H; t; J = 4.2; piperazine- $H^{2,6}$), 3.18 (4H; t; J = 4.2; piperazine- $H^{3,5}$), 3.36 (2H; s; piperidine-CH₂-pyran), 3.72 (2H; s; pyran-CH₂-piperazine); 6.49 (1H; s; pyran- H^5), 6.81 (2H; dd; $J_1 = 2.4$; $J_2 = 6.8$; Ar- $H^{2,6}$), 7.19 (2H; dd; $J_1 = 2.4$; $J_2 = 6.8$ Ar- $H^{3,5}$); ¹³C NMR (CDCl₃, 100 MHz) δ ppm: 23.90, 25.88 (piperidine- $C^{3,4,5}$), 49.09, 52.73 (piperazine- $C^{2,3,5,6}$), 54.59 (piperidine- $C^{2,6}$), 54.81 (piperazine-C), 60.30 (piperidine-C), 111.20 (pyran-C⁵), 117.36, 124.77, 128.97 (4-chlorobenzene- $C^{2,3,4,5,6}$), 143.80 (pyran- C^2), 145.27 (pyran- C^3), 149.70 (4-chlorobenzene- C^1), 165.99 (pyran- C^6), 173.93 (pyran- C^4); ESI-MS (m/z): 418 (100%, M⁺+H), 420 $(M^++H+2).$

2-((4-(3,4-Dichlorophenyl)piperazine-1-yl)methyl)-3-hydroxy-6-(piperidine-1-ylmethyl)-4*H*-pyran-4-one

(4d): C₂₂H₂₇Cl₂N₃O₃.M.W.: 452.374 g/mol; Yield: 18%; mp: 156-158 °C; %CHN Found (Calculated): C 57.98 (58.41), H 6.13 (6.02), N 9.30 (9.29); IR υ (cm⁻¹): 1620 (C=O, st), 1484, 1454 (C=C, st), 2938 (C-H, st, aliphatic), 1596 (C-C (in-ring), st), 1240, 1202 (C-N, st), 1010 (C-O, st); ¹H NMR (CDCl₃, 400 MHz) δ ppm: 1.43 (2H; m; piperidine- H^4), 1.58 (4H; m; piperidine- $H^{3,5}$), 2.45 (4H; t; J =5,6; piperidine- $H^{2,6}$), 2.72 (4H; t; J = 5,2; piperazine- $H^{2,6}$), 3.18 (4H; t; J = 5.2; piperazine- $H^{3.5}$), 3.36 (2H; s; piperidine-CH₂-pyran), 3.71 (2H; s; pyran-CH₂-piperazine), 6.49 (1H; s; pyran- H^5), 6.71 (1H; dd; $J_1 = 2.8$; $J_2 = 9.2$; Ar-H⁶), 6.93 (1H; d; J = 2.4; Ar-H²), 7.25 (1H; d; J = 8; Ar- H^5); ¹³C NMR (CDCl₃, 100 MHz) δ ppm: 23.88 and 25.85 (piperidine- $C^{3,4,5}$), 48.57, 52.52 (piperazine- $C^{1,2,4,5}$), 54.57 (piperidine-C^{2,6}), 54.60 (piperazine-C), 60.30 (piperidine-C), 111.20 (pyran-C⁵), 115.40, 117.34, 122.36, 130.44, 132.78 (3,4-dichlorobenzene-C^{2,3,4,5,6}), 143.81 (pyran- C^2), 145.30 (3,4-dichlorobenzene- C^1), 150.46 (pyran- C^3), 166.00 (pyran- C^6), 173.96 (pyran- C^4); ESI-MS (m/z): 222 (100%), 452 (M^++H) , 454 (M^++H+2) , 456 $(M^{+}+H+4).$

2-((4-Phenylpiperazine-1-yl)methyl)-3-hydroxy-6-(3methylpiperidine-1-ylmethyl)-4H-pyran-4-one C₂₃H₃₁N₃O₃. M.W.: 397.511 g/mol; Yield: 47%; mp: 149-150 °C; %CHN Found (Calculated): C 69.50 (69.49), H 7.72 (7.86), N 10.56 (10.57); IR v (cm⁻¹): 1620 (C=O, st), 1503, 1455 (C=C, st), 2928 (C-H, st, aliphatic), 1597 (C-C (in-ring), st), 1238, 1200 (C-N, st), 1003 (C-O, st); ¹H NMR (CDCl₃, 400 MHz) δ ppm: 0.85 (3H; d; J = 6; -CH₃), 1.57–1.76 (5H; m; piperidine- $H^{3,4,5}$), 2.04 (1H; td; J = 3.2; J= 10.8; piperidine- H^6), 2.75–2.82 (7H; m; piperidine- $H^{2,6}$, piperazine- $H^{2,6}$), 3.22 (4H; t; J = 4.2; piperazine- $H^{3,5}$), 3.39 (2H; s; piran-CH₂-piperidine), 3.74 (2H; s; pyran-CH₂-piperazine), 6.50 (1H; s; pyran- H^5), 6.86 (1H; t; $I_1 = 7.2$; $I_2 =$ 14.4; Ar- H^4), 6.91 (2H; d; J = 8; Ar- $H^{2,6}$), 7.26 (2H; t; $J_1 =$ 6.4; $J_2 = 10$; Ar- $H^{3,5}$); ¹³C NMR (CDCl₃, 100 MHz) δ ppm: 19.53 (CH₃), 25.39, 31.11, 32.47 (piperidine-C^{3,4,5}), 49.12, 52.90 (piperazine- $C^{1,2,4,5}$), 54.02 (piperidine- C^6), 54.99 (piperazine-C), 59.97 (piperidine-C), 61.83 (piperidine- C^2), 111.33 (pyran- C^5), 116.22, 119.97, 129.13 (benzene- $C^{2,3,4,5,6}$), 143.86 (pyran- C^2), 145.35 (pyran- C^3), 151.08 (benzene- C^1), 165.81 (pyran- C^6), 173.96 (pyran- C^4); ESI-MS (m/z): 163 (100%), 398 M⁺+H).

2-((4-(4-Fluorophenyl)piperazine-1-yl)methyl)-3-hydroxy-6-(3-methylpiperidine-1-ylmethyl)-4*H*-pyran-4-one (4f): C₂₃H₃₀FN₃O₃.1/2 CH₃OH. M.W.: 415.501 g/mol; Yield: 27%; mp: 130–131 °C; %CHN Found (Calculated): C 65.88 (65.76), H 7.25 (7.41), N 10.05 (9.86); IR ν (cm⁻¹): 1627 (C=O, st), 1510, 1455 (C=C, st), 2937 (C-H, st, aliphatic), 1244, 1199 (C-N, st), 1003 (C-O, st); ¹H NMR (CDCl₃, 400 MHz) δ ppm: 0.85 (3H; d; J = 6.4; - CH_3), 1.57–1.76 (5H; m; piperidine- $H^{3,4,5}$), 2.03 (1H; td; $J_1 = 3.2$; $J_2 = 11.8$ piperidine- H^6), 2.75–2.82 (7H; m; piperidine- $H^{2,6'}$, piperazin- $H^{2,6}$), 3.12 (4H; t; J = 5.2; piperazine- $H^{3,5}$), 3.38

(2H; s; pyran- CH_2 -piperidine), 3.72 (2H; s; pyran- CH_2 -piperazine), 6.49 (1H; s; pyran- H^5), 6.86 (2H; m; Ar- $H^{2,6}$), 6.95 (2H; m; Ar- $H^{3,5}$); ¹³C NMR (CDCl₃, 100 MHz) δ ppm: 19.51 (CH_3), 25.36, 31.08, 32.46 (piperidine- $C^{3,4,5}$), 50.10, 52.88 (piperazine- $C^{1,2,4,5}$), 54.02 (piperidine- C^6), 54.88 (piperazine-C), 59.99 (piperidine-C), 61.83 (piperidine- C^2), 111.34 (pyran- C^5), 115.54 (d, J = 20, 4-fluorobenzene- $C^{3,5}$), 118.00 (d, J = 10, 4-fluorobenzene- $C^{2,6}$), 143.82 (pyran- C^2), 145.27 (pyran- C^3), 147.74 (d, J = 1, 4-fluorobenzene- C^I), 157.29 (d, J = 250, 4-fluorobenzene- C^I), 165.79 (pyran- C^6), 173.95 (pyran- C^4); ESI-MS (m/z): 416 (100%, M^+ +H).

2-((4-(4-Chlorophenyl)piperazine-1-yl)methyl)-3-hydroxy-6-(3-methylpiperidine-1-ylmethyl)-4H-pyran-4one (4g): C₂₃H₃₀ClN₃O₃.1/2 CH₃OH. M.W.: 431.956 g/ mol; Yield: 34%; mp: 142-143°C; %CHN Found (Calculated): C 62.86 (63.01), H 6.89 (7.20), N 9.57 (9.38); IR v (cm⁻¹): 1626 (C=O, st), 1497, 1455 (C=C, st), 2931 (C-H, st, aliphatic), 1598 (C-C (in-ring), st), 1244, 1201 (C-N, st), 1000 (C–O, st); ¹H NMR (CDCl₃, 400 MHz) δ ppm:) 0.86-0.84 (3H; d; J = 6; $-CH_3$), 1.57-1.73 (5H; m; piperidine- $H^{3,4,5}$), 2.02 (1H; td; $J_1 = 3.2$; $J_2 = 11.2$; piperidine- H^6), 2.74-2.82 (7H; m; piperidine- $H^{2,6}$, piperazine- $H^{2,6}$), 3.18 $(4H; t; J = 5.2; piperazine-H^{3,5}), 3.38 (2H; s; pyran-CH₂-pip$ eridine), 3.73 (2H; s; pyran- CH_2 -piperazine), 6.50 (1H; s; pyran- H^5), 6.82 (2H; dd; $J_1 = 2$; $J_2 = 7.2$; Ar- $H^{2,6}$), 7.19 (2H; dd; $J_1 = 2$; $J_2 = 7.2$; Ar- $H^{3,5}$); ¹³C NMR (CDCl₃, 100 MHz) δ ppm: 19.51 (- CH_3), 25.36, 31.08, 32.46 (piperidine- $C^{3,4,5}$), 49.10, 52.73 (piperazine- $C^{1,2,4,5}$), 54.03 (piperidine- C^6), 54.82 (piperazine-C), 59.98 (piperidine-C), 61.83 (piperidine-C²), 111.27 (pyran-C⁵), 117.37, 124.78, 128.97 $(4-\text{chlorobenzene-}C^{2,3,4,5,6}), 143.82 \text{ (pyran-}C^2), 145.27$ $(4-\text{chlorobenzene-}C^1), 149.69$ (pyran- C^3), 165.86 (pyran- C^6), 173.93 (pyran- C^4); ESI-MS (m/z): 217 (% 100), 432 (M++H), 434 (M++H+2).

2-((4-(3,4-Dichlorophenyl)piperazine-1-yl)methyl)-3hydroxy-6-(3-methyl piperidine-1-ylmethyl)-4H-pyran -4-one (4h): C₂₃H₂₉Cl₂N₃O₃ .1/2 CH₃OH. M.W.: 466.401 g/mol; Yield: 77%; mp: 169-171 °C; %CHN Found (Calculated): C 58.37 (58.51), H 6.18 (6.48), N 8.98 (8.71); IR v (cm⁻¹): 1628 (C=O, st), 1485, 1453 (C=C, st), 2932 (C-H, st, aliphatic), 1596 (C-C (in-ring), st), 1237, 1199 (C-N, st), 1000 (C–O, st); ^1H NMR (CDCl $_3$, 400 MHz) δ ppm: 0.85 (3H; d; I = 6; -CH₃), 1.60-1.74 (5H; m; piperidine- $H^{3,4,5}$), 2.03 (1H; td; $J_1 = 3.2$; $J_2 = 10.8$; piperidine- H^6), 2.72-2.82 (7H; m; piperidine- $H^{2,6}$, piperazine- $H^{2,6}$), 3.19 $(4H; t; J = 5.2; piperazine-H^{3,5}), 3.39 (2H; s; pyran-CH₂-pip$ eridine), 3.72 (2H; s; pyran- CH_2 -piperazine), 6.50 (1H; s; pyran- H^5), 6.71 (1H; dd; J = 2.4; J = 8.8; Ar- H^6), 6.93 (1H; d; J = 2.4; Ar- H^2), 7.25 (1H; d; J = 2.4; Ar- H^6); ¹³C NMR (CDCl₃, 100 MHz) δ ppm: 19.51 (CH₃), 25.33, 31.07, 32.43 (piperidine- $C^{3,4,5}$), 48.60, 52.53 (piperazine- $C^{1,2,4,5}$), 54.30 (piperidine- C^6), 54.66 (piperazine-C), 59.98 (piperidine-C), 61.82 (piperidine- C^2), 111.24 (pyran- C^5), 115.40, 117.35, 122.38, 130.45, 132.80 (3,4-dichlorobenzene- $C^{2,3,4,5,6}$), 143.80 (pyran- C^2), 145.24 (3,4-dichlorobenzene- C^1), 150.46 (pyran- C^3), 165.88 (pyran- C^6), 173.90 (pyran- C^4); ESI-MS (m/z): 234 (100%), 466 (M⁺+H), 468 (M⁺+H+2), 470 (M⁺+H+4).

2-((4-Phenylpiperazine-1-yl)methyl)-3-hydroxy-6-(4methylpiperidine-1-ylmethyl)-4H-pyran-4-one C₂₃H₃₁N₃O₃.M.W.: 397.511 g/mol; Yield: 44%; mp: 148-149 °C; %CHN Found (Calculated): C 69.11 (69.49), H 7.75 (7.86), N 10.48 (10.57); IR v (cm⁻¹): 1617 (C=O, st), 1503, 1455 (C=C, st), 2915 (C-H, st, aliphatic), 1597 (C-C (in-ring), st), 1240, 1201 (C-N, st), 1001 (C-O, st); ¹H NMR (CDCl₃, 400 MHz) δ ppm: 0.92 (3H; d; I = 6; -CH₃), 1.21–1.37 (3H; m; piperidine- $H^{3,4,5}$), 1.62 (2H; d; J = 12; piperidine- $H^{3,5}$), 2.11 (2H; t; J = 11.2; piperidine- $H^{2,6}$), 2.77 (4H; t; I = 5.2; piperazine- $H^{2,6}$), 2.85 (2H; d; I = 11.2; piperidine- $H^{2,6}$), 3.22 (4H; t; J = 5.2; piperazine- $H^{3,5}$), 3.40 (2H; s; pyran-CH₂-piperidine), 3.74 (2H; s; pyran- CH_2 -piperazine), 6.49 (1H; s; pyran- H^5), 6.87 (1H; t; J = 6.8; Ar- H^4), 6.92 (2H; d; J = 8.4; Ar- $H^{2,6}$), 7.26 (2H; t; J = 9.2; Ar- $H^{3,5}$); ¹³C NMR (CDCl₃, 100 MHz) δ ppm: $21.76 (-CH_3)$, 30.36, 34.16 (piperidine- $C^{3,4,5}$), 49.11, 52.89(piperazine- $C^{1,2,4,5}$), 53.98 (piperidine- $C^{2,6}$), 55.02 (piperazine-C), 59.87 (piperidine-C), 111.39 (pyran- C^5), 116.22, 119.98, 129.13 (benzene- $C^{2,3,4,5,6}$), 143.86 (pyran- C^2), (pyran- C^3), 151.07 (benzene- C^1), 165.78 (pyran- C^6), 173.93 (pyran- C^4); ESI-MS (m/z): 163 (% 100), 398 (M++H).

2-((4-(4-Fluorophenyl)piperazine-1-yl)methyl)-3-hydroxy-6-(4-methylpiperidine-1-ylmethyl)-4H-pyran-4one (4j): C₂₃H₃₀FN₃O₃.M.W.: 415.501 g/mol; Yield: 33%; mp: 161-163 °C; %CHN Found (Calculated): C 66.10 (66.49), H 7.25 (7.28), N 10.01 (10.11); IR υ (cm⁻¹): 1619 (C=O, st), 1509, 1455 (C=C, st), 2929 (C-H, st, aliphatic), 1597 (C-C (in-ring), st), 1240, 1200 (C-N, st), 999 (C-O, st); ¹H NMR (CDCl₃, 400 MHz) δ ppm: 0.92 (3H; d; J = 6; $-CH_3$), 1.24–1.35 (3H; m; piperidine- $H^{3,4,5}$), 1.61 (2H; d; J =12.8; piperidine- $H^{3',5'}$), 2.10 (2H; t; J = 9.6; piperidine- $H^{2,6}$), 2.76 (4H; t; J = 4.2; piperazine- $H^{2,6}$), 2.85 (2H; d; J = 12; piperidine- $H^{2',6'}$), 3.14 (4H; t; J = 4.2; piperazine- $H^{3,5}$), 3.39 (2H; s; pyran- CH_2 -piperidine), 3.73 (2H; s; pyran- CH_2 -piperazine), 6.49 (1H; s; pyran- H^5), 6.84–6.87 (2H; m; Ar- $H^{2,6}$), 6.93–6.97 (2H; m; Ar- $H^{3,5}$); ¹³C NMR (CDCl₃, 100 MHz) δ ppm: 21.76 (- CH_3), 30.37, 34.17 (piperidine- $C^{3,4,5}$), 50.13, 52.88 (piperazine- $C^{2,3,5,6}$), 53.99 (piperidine- $C^{2,6}$), 54.94 (piperazine-C), 59.879 (piperidine-C), 111.362 (pyran- C^5), 115.56 (d, J = 20, 4-fluorobenzene- $C^{3,5}$), 118.01 (d, J = 10, 4-fluorobenzene- $C^{2,6}$), 143.85 (pyran- C^2), (pyran- C^3), 147.74 (d, J = 1, 4-fluorobenzene- C^1); 157.30 $(d, I = 250, 4-fluorobenzene-C^4)$; 165.82 (pyran-C⁶), 173.93 (pyran- C^4); ESI-MS (m/z): 416 (100%, M⁺+H).

2-((4-(4-Chlorophenyl)piperazine-1-yl)methyl)-3-hydroxy-6-(4-methylpiperidine-1-ylmethyl)-4*H*-pyran-4-

one (4k): C₂₃H₃₀ClN₃O₃.1/2 CH₃OH. M.W.: 431.956 g/ mol; Yield: 31%; mp: 161-163 °C; %CHN Found (Calculated): C 63.07 (63.01), H 6.89 (7.20), N 9.60 (9.38); IR v (cm⁻¹): 1628 (C=O, st), 1497, 1455 (C=C, st), 2919 (C-H, st, aliphatic), 1599 (C-C (in-ring), st), 1242, 1200 (C-N, st), 1005 (C–O, st); ¹H NMR (CDCl₃, 400 MHz) δ ppm: 0.91 (3H; d; J = 6.4; - CH_3), 1.22–1.34 (3H; m; piperidine- $H^{3,4,5}$), 1.61 (2H; d; J = 12.8; piperidine- $H^{3,5}$), 2.08 (2H; t; J = 11.2; piperidine- $H^{2,6}$), 2.74 (4H; t; J = 4.2; piperazine- $H^{2,6}$), 2.83 (2H; d; J = 12.8; piperidine- $H^{2,6}$), 3.17 $(4H; t; J = 4.2; piperazine-H^{3,5}), 3.37 (2H; s; pyran-CH₂-pip$ eridine), 3.72 (2H; s; pyran- CH_2 -piperazine), 6.48 (1H; s; pyran- H^5), 6.79–6.81 (2H; dd; $J_1 = 2.4$; $J_2 = 6.8$; Ar- $H^{2,6}$), 7.18 (2H; dd; $J_1 = 2$; $J_2 = 4.4$; Ar- $H^{3,5}$); ¹³C NMR (CDCl₃) 100 MHz) δ ppm: 21.75 (-CH₃), 30.374, 34,18 (piperidine- $C^{3,4,5}$), 49.07, 52.72 (piperazine- $C^{2,3,5,6}$), 54.01 (piperidine- $C^{2,6}$), 54.78 (piperazine-C), 59.97 (piperidine-C), 111.26 (pyran-C⁵), 117.35, 124.51, 128.96 (4-chlorobenzene-C^{2,3,4,5,6}), 143.83 (pyran-C²), 145.31 (4-chlorobenzene- C^1), 149.69 (pyran- C^3), 165.95 (pyran- C^6), 173.95 (pyran- C^4); ESI-MS 432 (100%, M⁺+H), 434 (M⁺+2).

2-((4-(3,4-Dichlorophenyl)piperazine-1-yl)methyl)-3hydroxy-6-(4-methylpiperidine-1-ylmethyl)-4H-pyran-**4-one** (**4l**): C₂₃H₂₉Cl₂N₃O₃.CH₃OH. M.W.: 466.401 g/mol; Yield: 66%; mp: 154-155 °C; %CHN Found (Calculated): C 57.96 (57.83), H 6.29 (6.67), N 8.87 (8.43); IR υ (cm⁻¹): 1631 (C=O, st), 1485, 1453 (C=C, st), 2916 (C-H, st, aliphatic), 1631 (C=O, st), 1596 (C-C (in-ring), st), 1237, 1198 (C-N, st), 1001 (C-O, st); ¹H NMR (CDCl₃, 400 MHz) δ ppm: 0.91 (3H; d; J = 6.4; - CH_3), 1.22–1.34 (3H; m; piperidine- $H^{3,4,5}$), 1.60 (2H; d; J = 13.2; piperidine- $H^{3,5}$), 2.08 (2H; td; $J_1 = 11.6$; $J_2 = 2.4$; piperidine- $H^{2,6}$), 2.72 (4H; t; J = 5.2; piperazine- $H^{2,6}$), 2.83 (2H; d; J = 12.4; piperidine- $H^{2',6'}$), 3.18 (4H; t; J = 5,2 piperazine- $H^{3,5}$), 3.37 (2H; s; pyran-CH₂-piperidine), 3.71 (2H; s; pyran-CH₂-piperazine), 6.48 (1H; s; pyran- H^5), 6.71 (1H; dd; $J_1 = 3.2$; $J_2 = 9.2$; Ar- H^6), 6.93 (1H; d; J = 2.8; Ar- H^2), 7.24 (1H; d; J = 9.2; Ar- H^5); ¹³C NMR (CDCl₃, 100 MHz) δ ppm: 21.75 (- CH_3), 30.38, 34.18 (piperidine- $C^{3,4,5}$), 48.58, 52.52 (piperazine- $C^{1,2,4,5}$), 54.01 (piperidine- $C^{2,6}$), 54.61 (piperazine-C), 59.97 (piperidine-C), 111.20 (pyran-C⁵), 115.40, 117.34, 122.35, 130.44, 132.78 (3,4-dichlorobenzene- $C^{2,3,4,5,6}$), 143.80 (pyran- C^2), 145.26 (3,4-dichlorobenzene- C^1), 150.46 (pyran- C^3), 166.05 (pyran- C^6), 173.93 (pyran- C^4); ESI-MS (m/z): 466 (100%, M++H), 468 (M++H+2), 470 $(M^++H+4).$

2. 2. Biochemistry

2. 2. 1. Cell culture

The B16F10 mus musculus skin melanoma cell line (ATCC* CRL-6475™) was purchased from the American Type Culture Collection (ATCC). Cells were routinely maintained in RPMI-1640 medium containing 10% heat-inactivated fetal bovine serum, 2 mM L-glutamine,

100 U/mL penicillin/streptomycin (Gibco) in a humidified incubator (Panasonic MCO-18 AC-PE) with 5% $\rm CO_2$ at 37 °C.

2. 2. 2. Tyrosinase Inhibition of Compounds

To determine the mushroom tyrosinase inhibitory potential of the newly synthesized compounds, the oxidation rate of L-DOPA was measured spectrophotometrically²⁶ and compared with the inhibition of KA. Briefly, the reaction mixture contained 100 µL 50 mM phosphate buffer (pH 6.8), 10 μL of inhibitor/ dimethyl sulfoxide (DMSO), and 10 µL of mushroom tyrosinase (Sigma, T3824). The samples containing DMSO were considered control groups. Kojic acid, a strong inhibitor of mushroom tyrosinase, was used as a positive control. The reaction mixture was preincubated for 20 min at 37 °C and the reaction was initiated with the addition of 30 μL of 5 mM L-DOPA (Sigma, D9628). Following 20 min of incubation at 37 °C, the absorbance values of the samples were obtained at 492 nm using an ELISA Plate Reader (BioTek PowerWave). By subtracting the values recorded by DMSO addition only, the % inhibition was calculated. Increasing concentrations of each compound (8-2000 µM) were tested in quadruplicates and the IC₅₀ values were determined by constructing a nonlinear regression curve. The IC₅₀ value of mushroom tyrosinase inhibition for each compound is presented in Table 2.

2. 2. 3. Cytotoxicity Assay

To determine the cytotoxicity of newly synthesized compounds and Dacarbazine in the B16F10 cell line, the Sulforhodamine B (SRB) assay was performed. According to the colorimetric end-point method described by Vichai and Kirtikara²⁷, cells were first inoculated in 96-well plates at 2×10³ cells/well density. At confluency, increasing concentrations of the compounds and Dacarbazine were applied for 48 hours. 10% (w/v) trichloroacetic acid (TCA, Sigma-Aldrich, USA) was used to fix the cells for 2 hours at 4 °C. Cells were washed several times with dH₂O, then 0.06% (w/v) SRB dye (Santa Cruz Biotechnology, USA) was applied for 30 minutes at room temperature and the excess dye was removed with 1% (v/v) acetic acid (Sigma-Aldrich). Finally, the samples were resuspended in 200 μL Tris base (10 mM, pH 10.5), and the optical density (OD) was measured at 510 nm using a microplate reader (PowerWave XS, Biotek). Untreated cells were regarded as a control and were 100% viable. OD values obtained from treated wells were compared to the control, cytotoxicity percentage, and the IC50 values were calculated for each cell line.

2. 2. 4. Melanogenesis Inhibition Assay

B16F10 mus musculus skin melanoma cells were seeded in 6-well plates at 5×10^5 cells/well density.²⁴ At 90%

confluency, Kojic acid and selected compounds having tyrosinase inhibition potential were applied at their IC_{50} doses and incubated for 48 hours. Collected cells were lysed and sonicated 5 times at 30% amplitude for 10 seconds each. Cells were centrifuged at 12000 rpm, at 37 °C, for 5 min. 10% TCA and 75% EtOH were used to wash the pellets, and 0.25 N NaOH containing 2.5 % DMSO was added. The samples were then incubated for 1 hour at 80 °C in a water bath. Samples were measured spectrophotometrically at 470 nm, where the absorbance of the untreated sample was designated as the control group. The samples were run in triplicate and the results were calculated as % of the melanin content.

2. 3. Statistical Analysis

GraphPad Prism 5.03 software was used to evaluate all statistical analyses. A non-linear regression model was used to calculate the IC_{50} values of the compound and Dacarbazine in B16F10 cells. Mann–Whitney U test was used to compare all data to their related control. All p-values were based on the two-sided statistical analysis, and p < 0.05 was considered to be statistically significant. All experiments were carried out at least in triplicate.

2. 4. Molecular Docking Analysis

The crystal structure of mushroom tyrosinase enzyme with PDB ID of 2X9Y was used for molecular modeling assays. The binding site was defined based on previously reported active site residues, as described²⁶ and confirmed by literature data regarding the catalytic site of the enzyme. Therefore, the docking was performed in the active site region.

Docking studies were performed for the most active three compounds, **4b**, **4j**, and **4l**, against the mushroom tyrosinase enzyme. Grid parameters for AutoDock Vina were set to cover the catalytic pocket of the enzyme, where the oxidation of phenolic substrates typically occurs. Ligands were prepared by using Biovia Discovery Studio Visualizer and MGLTools software. The ionization ratios of the compounds at physiological pH were evaluated, and the 1st atoms of piperidine and piperazine rings were prepared as positively charged. As the 4th atom of the piperazine ring is substituted with a phenyl ring, it was kept neutral. AutoDock Vina docking tool was used to predict the possible binding modes of the selected compounds. Binding conformations of each of the three were evaluated with Biovia Discovery Studio Visualizer.

2. 5. Preparation of Test, Prediction, and Validation Sets

The chemical structures of compounds were prepared as mol files using ChemDraw and converted to sdf format using Openbabbel software. For each of the test, prediction, and validation sets, the structures of the compounds were merged into a single SDF file using Data Warrior. The molecular descriptors for each set were calculated using the CDK calculator. All the descriptors available in the software package were selected, including hybrid, constitutional, topological, electronic, and geometric descriptors.

2. 6. Computer-Aided Drug Design using Weka

QSAR models were constructed using Weka software. 28 The calculated molecular descriptors of the test set and the tyrosine activity (IC $_{50}$) values were imported into the program. The Classifier module was used to construct the prediction models. The models that showed the best performance were selected for the design of new compounds. The molecular descriptors of the prediction set were imported into Weka, and the selected models were used to predict the tyrosinase activities of the compounds. Compounds that were predicted to have good activities were selected for synthesis.

3. Results and Discussion

3. 1. Chemistry

To construct prediction models for tyrosine inhibitory action, descriptors were generated using the CDK software. A total of 287 descriptors were calculated, of which 171 were selected for model construction. Next, the Weka software package was used to construct the prediction models. This software package introduces base models using confusion matrices.²⁸ Regression involves the construction of a model that uses mathematical functions to correlate between instances labeled with continuous variables that are defined by a set of selected attributes. 16 The test set included 25 compounds with previously reported anti-tyrosinase activities.²⁶ Table 1 shows the results of the eight models developed using WEKA. All models performed well on the test set, with correlations (r²) ranging from 0.753 to 1. Accordingly, we designed twelve 2-(4-(substituted phenyl) piperazine-1-yl) meth-

Table 1. Performances and predictive abilities of eight QSAR models

	Method	\mathbf{r}^2	\mathbf{q}^2
1	Multilayer perceptron	1	0.12
2	IBK	1	0.20
3	Additive regression	1	0.19
4	Bagging	0.71	0.50
5	Random committee	1	0.50
6	Random SubSpace	0.81	0.20
7	Regression By Discretization	0.75	0.45
8	Decision table	0.98	0.56

yl-3-hydroxy-6-(piperidin/3-methylpiperidin/4-methyl piperidin) methyl-4*H*-pyran-4-one derivatives. Using the same molecular descriptors, the activities of the newly designed compounds were predicted by applying eight models using WEKA software.

The program predicted that all the compounds had good tyrosinase inhibitory activity. Therefore, all twelve novel compounds were synthesized according to the procedure shown in Figure 1. Structural modifications of the compound were made in two positions of the main hydroxypyranone skeleton. The $2^{\rm nd}$ position of the ring was modified by the Mannich reaction with appropriate phenylpiperazine moieties. Also, piperidine derivatives were substituted in the $6^{\rm th}$ position in the basic medium with piperidine derivatives.

Firstly, chlorokojic acid (2) was synthesized via the chlorination of commercially available kojic acid (1). Additionally, four different Mannich bases were gained by reacting the obtained chlorokojic acid with phenyl piperazine groups containing various halogen groups. Further, the chlorine atom at position 6 of the Mannich bases was substituted with piperidine derivatives in the basic medium, resulting in the synthesis of twelve new compounds. These compounds were identified as 2-(4-(substituted phenyl)

piperazin-1-yl)methyl-3-hydroxy-6-(piperidine/3-methylpiperidine/4-methylpiperidine)methyl-4*H*-pyran-4-one.

The structures of the novel compounds were verified by using spectroscopic techniques and elemental analysis results. The yields of the reactions and melting points were given in monographs. The IR spectra selected diagnostic bands provided useful information to identify the hydroxypyrone skeleton. Two hydrogen bondings, both intra- and intermolecular, were observed in the hydroxymethyl moiety. The stretching of C=O (pyranone) gave signals at 1631–1618 cm⁻¹. In the IR spectra of all compounds, the stretching (st) bands associated with C=C and C-O were observed at about 1484-1455, and 999-1010 cm⁻¹, respectively. When examining the ¹H NMR spectra of compounds obtained in CDCl₃, the integral values confirm the presence of protons. The values of the hydrogens belonging to the hydroxypyrone nucleus, which is the common structure in all compounds, match each other in the ¹H NMR spectrum. The hydrogen attached to the carbon at position 5 of the ring is seen as a singlet in the range of 6.48–6.50 ppm. However, the OH peak in the pyrone ring was not observed in any of the compounds. This is because the hydrogens attached to the heteroatom are easily exchangeable with the deuterium atom in the solvent. In all

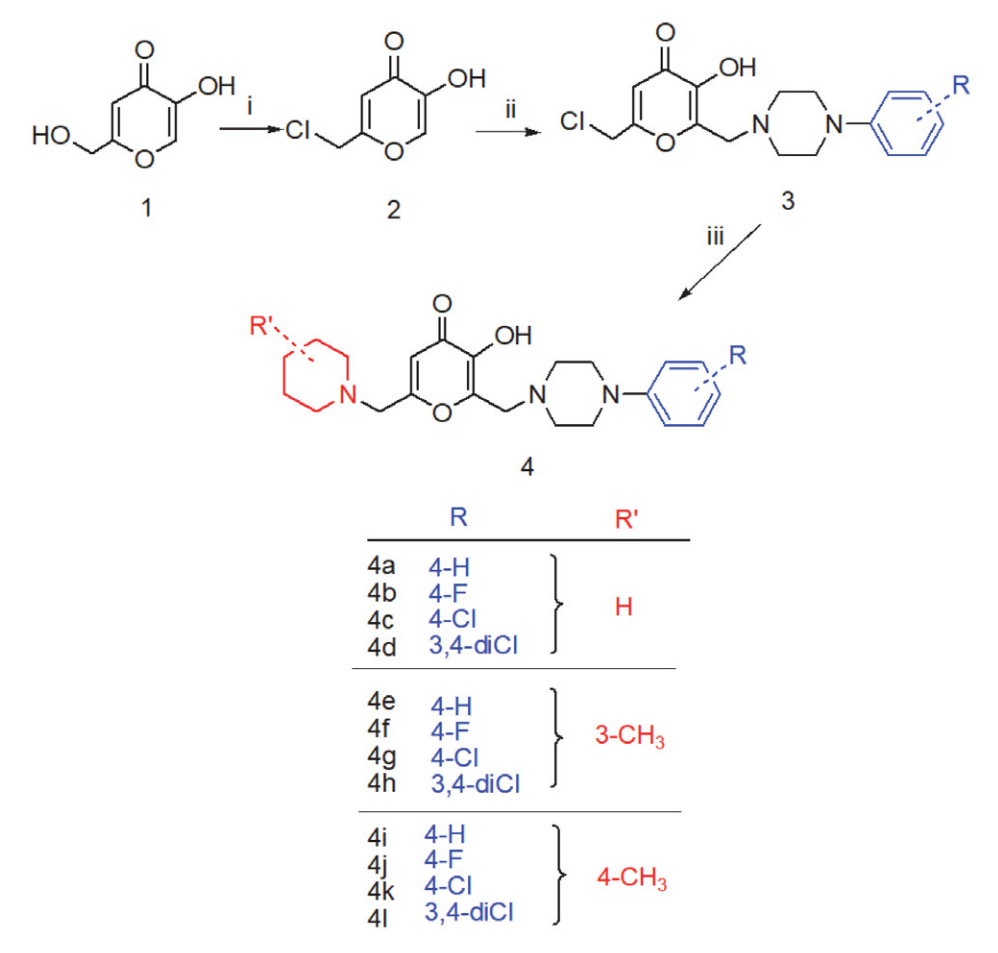


Figure 1. General synthesis of compounds 4a-l. Reagents, and conditions: i: $SOCl_2$, ii: HCHO, phenylpiperazine derivatives, in MeOH, rt; iii: piperidine derivatives, K_2CO_3 , DMF, 0°C

compounds, the peaks belonging to hydrogens attached to the carbons of the piperazine ring close to the pyrone ring were observed to peak in the range of 2.72-2.82 ppm, while hydrogens farther away gave peaks in the range of 3.12-3.72 ppm due to the decrease in the shielding effect in their chemical environment. Aromatic hydrogens of phenyl rings were at 6.71-7.26 ppm with suitable integral values. The 13 C NMR signals of compounds were in good agreement with the proposed structures. The carbon atom linked to the hydroxyl group on the third position of the pyranone ring (=C-OH) exhibited signals at 145-150 ppm. Carbonyl carbons of the 4H-pyran-4-one ring were found at 174 ppm. The mass spectra displayed molecular ion peaks and M^++23 (Na) peaks, indicating similar fragmentation patterns among the compounds.

3. 2. Mushroom Tyrosinase Inhibition

Two methods are commonly used to evaluate the tyrosinase inhibitory activity of compounds: *in vitro* mushroom tyrosinase assays and cell-based assays. During the *in vitro* test, a commercially available enzyme is employed as a model. As the enzyme can be easily used, it is extensively employed in the *in vitro* mushroom tyrosinase test. It also results in accurate data and enables scientists to focus on enzymological aspects. Most notably, the tyrosinase enzyme extracted from *A. bisporus* mushroom species is extremely similar to human ones; therefore, it is widely used for *in vitro* testing of melanogenesis.²⁹

The kinetic analysis of suppression of mushroom tyrosinase activity is substrate-specific. The method outlined by Chen³⁰ was used to evaluate the compounds' tyrosinase inhibitory activity with minor modifications. Each of the compounds was tested using a method that uses L-DOPA as the substrate. Kojic acid was employed as a positive control and also as a starting material for the synthesis process in this work. The examined inhibitory mechanism was based on tyrosinase's o-diphenolase activity. The IC $_{50}$ values and standard deviations were calculated using the GraphPad Prism 5.03 program. The IC $_{50}$ values of the compounds are shown in Table 2.

The effects of substitutions at positions 2 and 6 of the hydroxypyranone core on the antityrosinase activity of the synthesized compounds were investigated. In Mannich bases derived from position 2, the aromatic phenyl piperazine group is common and the phenyl ring is modified.

Nonsubstituted, a single halogen substituent at position 4 or 3,4-disubstituted derivatives were studied. When we divide the derivatives from the 6th position into three subgroups, the effects of methyl substitution on piperidine on antityrosinase activity can be interpreted.

We observed that the most effective compound among the synthesized compounds is **4l**, which carries a 3,4-dichloro group and nonsubstituted piperidine structures with an IC $_{50}$ value of 138.1 μ M. Furthermore, its 4-fluoro analog **4j** was found to be the second most active

compound, having an IC $_{50}$ value of 159.0 μ M. **4b** is the third most effective compound indicating that 4-fluoro substitution increases the tyrosinase inhibitory activity. These three molecules have higher inhibition values than the starting compounds used in synthesis and the control compound kojic acid (IC $_{50}=218~\mu$ M.). Dose-response curve for mushroom tyrosinase inhibitory activity of compound **4j** is given in Figure 2.

No correlation was found between the activity and adding halogens to the structure. However, in all three subgroups, the activity was significantly enhanced by the addition of the fluorine atom to the structure. This increase was particularly pronounced for the nonsubstituted piperidine and 4-methylpiperidine derivatives. Regarding the effect of the derivatization obtained from position 6, it can be inferred that the most effective group is the 4-methylpiperidine groups as they contain the two most active derivatives.

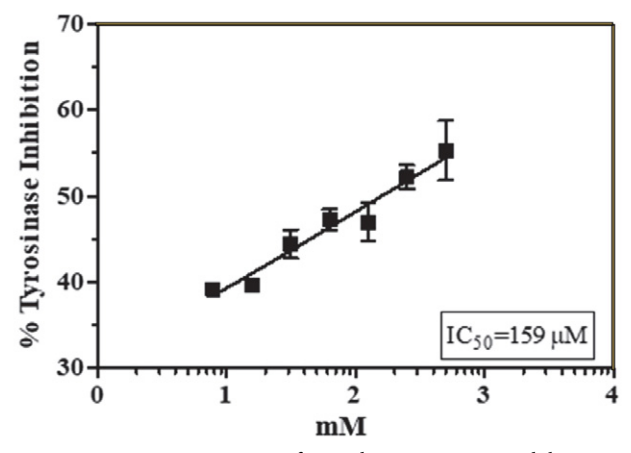


Figure 2. Dose-response curve for mushroom tyrosinase inhibitory activity of compound **4j.**

3. 3. Cytotoxicity of Compounds in B16F10 Cells

B16F10 mus musculus skin melanoma cells are suitable models for studying cytotoxicity due to their high metastatic potential. Unlike other melanoma cell lines,

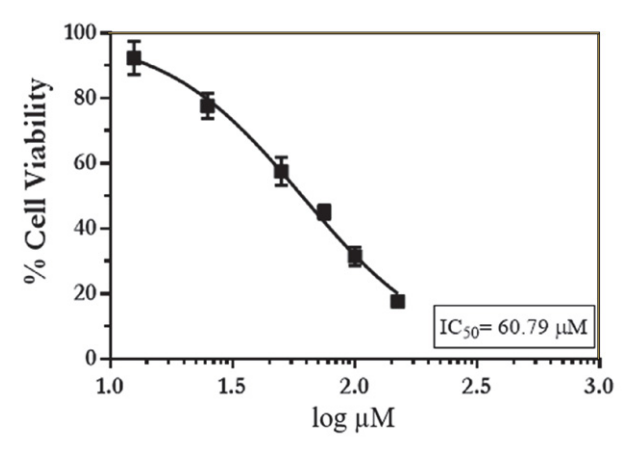


Figure 3. Dose-response curve for cytotoxicity of compound **4j** on B16F10 cells

they lack the BRAF mutation and maintain functional wild-type p53. The results showing the IC_{50} values of all tested compounds are shown in Table 2, and the dose-response curve for compound 4i is shown in Figure 3.

When the cytotoxic effects on B16F10 melanoma cells were evaluated, it was observed that compound 4c (19.35 μ M), having a non-substituted piperidine and a 4-chlorophenyl group, had the lowest IC₅₀ value. According to the decreasing activity, it is ranked as 4j, 4e, and 4b. It is noteworthy

and important that the IC_{50} values of eight compounds, including the starting materials and intermediates, were lower than the control compound dacarbazine ($IC_{50} = 110.8 \,\mu\text{M}$).

3. 4. Melanogenesis Assay in B16F10 Cells

Excessive melanin production can cause hyperpigmentation, leading to skin imperfections, spots, freckles, and even skin cancers. The melanin responsible for the

Table 2. Molecular formulas, structure, IC_{50} values of mushroom tyrosinase inhibition and cytotoxicity on B16F10 cells (IC_{50} as μM).

R'	OH N-R		
R'	R	Tyrosinase inhibition	Cytotoxicity
	seed of the seed o	1140	87.7
N—one —	sweet F	208.9	78.9
	₹ CI	1378	19.35
_	CI	nd	503.9
H ₃ C N - 5 -		1282	61.2
	F	1106	193.1
	CI	1870	nd
_	CI	nd	nd
H ₃ C — N — N — N — N — N — N — N — N — N —		nd	98.2
	Value F	159.0	60.8
	CI CI	nd	nd
	CI CI	138.1	nd
		218.8 296.6	98.8 71.7 110.8
	R' R' N washing -	R' R When the second s	R' R Tyrosinase inhibition 1140 208.9 1378 1282 106 11870 11870 1190

^{*}KA: Kojic acid; CKA: Chlorokojic acid; DAC: Dacarbazine

pigmentation of the skin and hair in humans is located at the basal layer of the epidermis. As a result, it is crucial to reverse hyperpigmentation by suppressing melanin production to treat these conditions. Tyrosinase inhibitors play a critical role in treating complications that arise from melanogenesis. Although Kojic acid is cytotoxic, it has limited effectiveness against melanogenesis on its own. Thus, it is essential to develop effective and less cytotoxic tyrosinase inhibitors. To quantify the impact of selected compounds and kojic acid on melanin formation in B16F10 cells, we measured the relative melanin content using spectrophotometry as described in the methods section. Due to their high melanocyte content, B16F10 mouse melanoma cells are an ideal model for studying melanogenesis. As discussed previously, compounds 4b and 4j were selected to evaluate melanogenesis suppression. Additionally, 4c was chosen due to its cytotoxic behavior over B16F10 cells. Results showed that 4j (82.8% inhibition) was significantly (p < 0.01) more effective than kojic acid (26.7% inhibition) in decreasing melanogenesis. Compounds 4b (24.7%) and 4c (49.1%) showed effects comparable to kojic acid. All assays were carried out in triplicate and the results were statistically analyzed. Given its anti-tyrosinase activity and cytotoxicity, 4j showed the highest anti-melanogenesis effect.

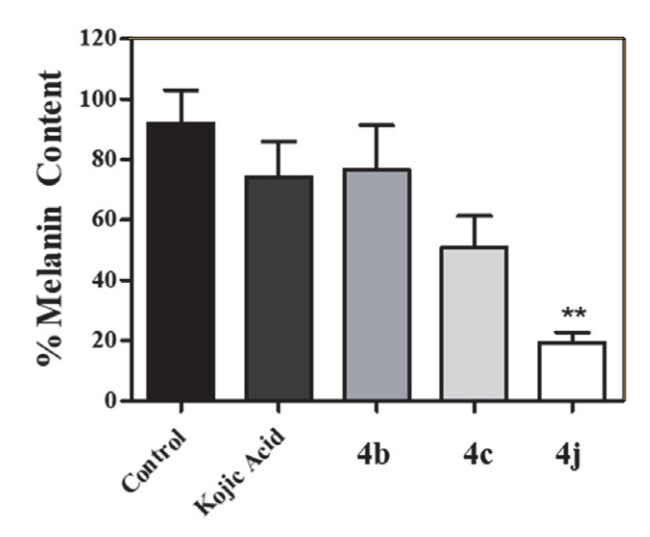


Figure 4. Effects of some compounds and kojic acid on melanogenesis on B16F10 cells. The melanin content was determined spectrophotometrically as described in the experimental section. Data (n=3) represent \pm mean SD.

3. 5. QSAR Analysis

A validation set that included the eight active compounds from the present study was constructed. The molecular descriptors were calculated using the CDK software and using the prediction models in Table 1 to validate them. Although all models showed good performance on the test set with correlations (r²) ranging from 0.753 to 1,

the majority of the models showed poor predictabilities when reapplied on the test. The best predictability was shown by the Decision tables method, which showed a q² value of 0.563, followed by the Bagging and Random Committee methods with q^2 values of 0.5. This implies these three methods are the most promising for the construction of models with excellent prediction performance. However, four compounds were falsely predicted to have activity using these models. This limitation in the performance of these models can be attributed to the small number of compounds that were used to construct them. Although the performance of these models can be considered satisfactory, better models can be constructed using larger datasets. Moreover, a multi-model approach can be applied in future datasets using ensemble learning with all three models. Such models will hopefully show better predictabilities, which will help in the design and development of tyrosine inhibitors for cosmetic and clinical applications.

3. 6. Molecular Docking Analysis

Computer-aided modeling studies were conducted to put more molecular insight into the tyrosinase inhibitory activity of the compounds **4b**, **4j**, and **4l**. In this concept, docking calculations were run considering the literature published.²² As docking studies were performed in the presence of copper ions, histidine amino acid residues that bind to copper ions were designated as 0HD1 forms. In consideration of the ionization states of the ligands, 1st atoms of piperidine and piperazine rings were kept positively charged. Conformations of the compounds **4b**, **4j**, and **4l** in the tyrosinase enzyme inhibition pocket were evaluated. Binding conformations of the compounds **4b**, **4j**, and **4l** in tyrosinase enzyme are presented in Figures 5–7.

As shown in Figure 5, the 3-hydroxy-4H-pyran-4-one ring interacts with Phe264 to form a π - π stacked interaction. The piperidine ring of compound **4b** formed several alkyl and π -alkyl interactions with His61, His85, Val283, and Ala286 amino acid residues. The piperidine ring also formed a carbon-hydrogen bond interaction with Ala260. The hydrogen atom of the protonated piperidine ring formed a π -cation interaction with His263. In addition, the 4-fluorophenyl substituent of compound **4b** makes carbon-hydrogen bond interaction with Asn81 and π -anion interaction with Glu322 amino acid residues. The fluro group in the phenyl ring forms halogen interaction with Ala323.

The conformation of compound **4j** in the tyrosinase enzyme pocket is presented in Figure 6. First, the 3-hydroxy-4*H*-pyran-4-one ring forms a conventional hydrogen bond with Asn260. The fluorine atom of the 4-fluorophenyl substituent of compound **4j** formed a carbon-hydrogen bond interaction with Asn81 amino acid. The fluoro group also interacts with Ala323. Carbon-hydrogen bond interactions were formed between the phenyl ring and Asn81, as well as between the piperazine ring and

His85. Protonated nitrogen atoms of piperidine and piperazine rings formed a π -cation interaction with His263 and an ionic interaction with Glu322, respectively. The methyl group at the 4th position of the piperidine ring forms hydrophobic interactions with His61, His85, Ala286, and Phe292 amino acids. π -sigma interactions can be seen between related methyl groups and His263 residue, additionally.

Figure 7 shows possible interactions between compound 4l and tyrosinase enzyme. As the hydrogen atom of protonated piperidine ring forms a hydrogen bond with Asn260, the 4-methyl substitution of the piperidine ring makes π -alkyl interactions with His61, His259, His263, and Val283 amino acid residues.

Val283 interacts with 3-hydroxy-4*H*-pyran-4-one ring as well. The protonated nitrogen atom of the pipera-

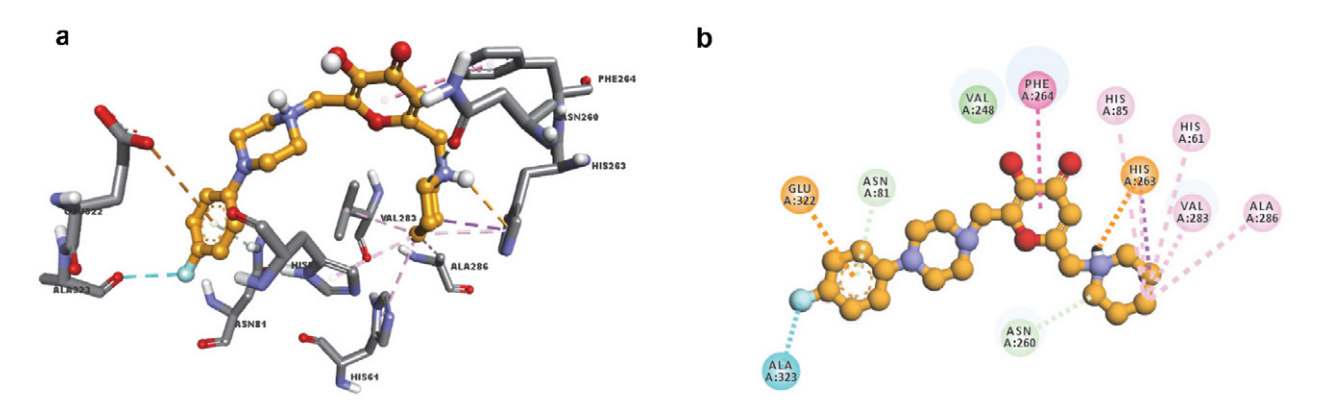


Figure 5. Molecular interactions between compound 4b and tyrosinase enzyme in 3D (a) and 2D (b). Compound 4b is shown as an orange ball and stick form.

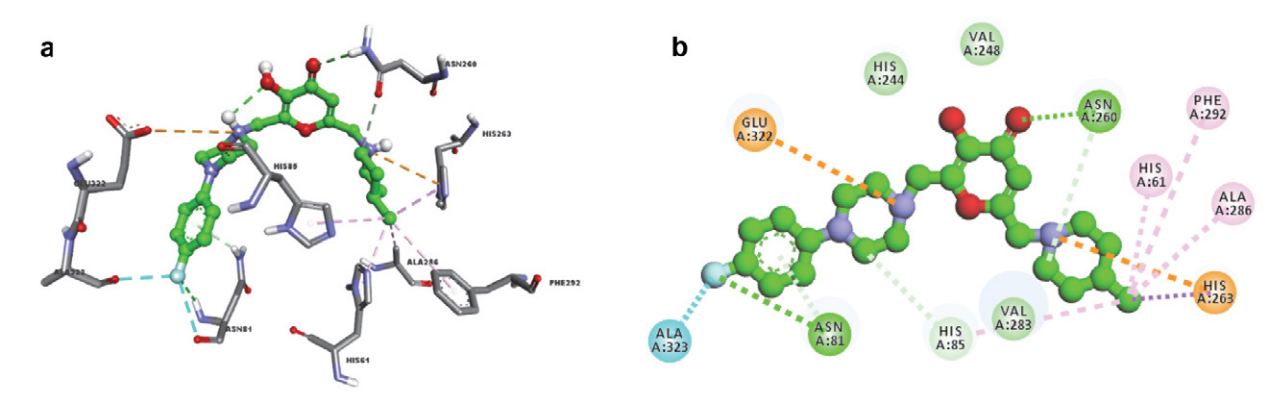


Figure 6. Molecular interactions between compound 4j and tyrosinase enzyme in 3D (a) and 2D (b). Compound 4j is represented as a green ball and stick form.

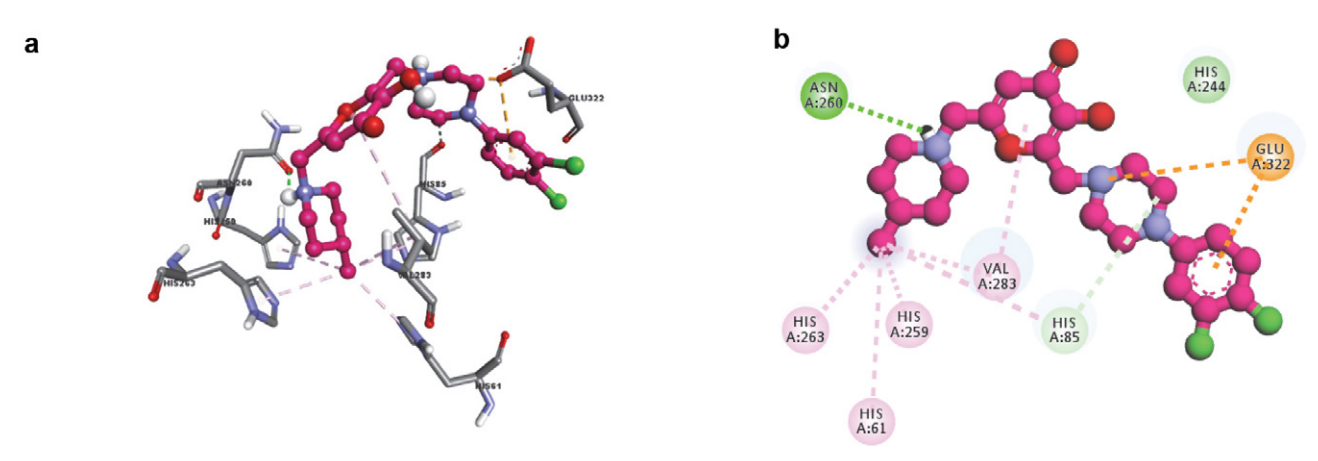


Figure 7. Molecular interactions between compound 4l and tyrosinase enzyme in 3D (a) and 2D (b). Compound 4l is represented as a pink ball and stick form.

zine ring makes cation-anion interaction with Glu322 amino acid. Glu322 also makes π -anion interaction with the phenyl ring. Piperazine ring makes carbon-hydrogen bond interaction with His85.

Consequently, possible interactions between tyrosinase protein and potential tyrosinase inhibitor compounds **4b**, **4j**, and **4l** are visualized in the current study. Modeling studies have shown that compounds having the 3-hydroxy-4*H*-pyran-4-one ring in the core structure can be oriented differently in the active site of the tyrosinase enzyme depending on the substitutions on this heterocyclic ring. Additionally, considering the ionization states, it can be suggested that heterocyclic piperidine and piperazine ring substitution on the structure may enhance inhibitory activity.

Val283 interacts with 3-hydroxy-4H-pyran-4-one ring as well. The protonated nitrogen atom of the piperazine ring makes cation-anion interaction with Glu322 amino acid. Glu322 also makes π -anion interaction with the phenyl ring. Piperazine ring makes carbon-hydrogen bond interaction with His85.

Consequently, possible interactions between tyrosinase protein and potential tyrosinase inhibitor compounds **4b**, **4j**, and **4l** are visualized in the current study. Modeling studies have shown that compounds having the 3-hydroxy-4*H*-pyran-4-one ring in the core structure can be oriented differently in the active site of the tyrosinase enzyme depending on the substitutions on this heterocyclic ring. Additionally, considering the ionization states, it can be suggested that heterocyclic piperidine and piperazine ring substitution on the structure may enhance inhibitory activity.

4. Conclusion

The objective of this research was to design and synthesize novel kojic acid derivatives bearing piperidine fragments possessing tyrosinase inhibitory activity with antimelanogenesis effect, using eight QSAR models. Also, their cytotoxic effects were aimed to investigate on B16F10 melanoma cells. In conclusion, compounds **4b** and **4j** were found to be the most active tyrosinase inhibitors, with compound **4j** showing higher inhibitory activity on melanogenesis than kojic acid. Compound **4c** exhibited the highest cytotoxicity to B16F10 melanoma cells, surpassing the clinically used control agent, dacarbazine. The findings of this study will shed light on the development of further candidates interacting directly with the active site of the enzyme, and as a convenient building block to achieve superior molecules.

Supporting Information

The Supporting information contains characterization of all compounds (FT-IR, ¹H NMR, and ¹³C NMR spectra).

Acknowledgements

This study was partially supported by the Hacettepe University Scientific Research Projects Coordination Unit (TYL-2018-17488, THD-2018-17033, THD-2015-7392). The authors thank Hacettepe University for their support.

Declarations

Conflict of interest The authors declare that they have no known competing financial interests or personal relationships that could have appeared to influence the work reported in this paper.

5. References

- S. Piña-Oviedo, C. Ortiz-Hidalgo, A. G. Ayala, *Arch. Path. Lab.* 2017, 141(3), 445–462. DOI:10.5858/arpa.2016-0274-SA
- I. Carballo-Carbajal, A. Laguna, J. Romero-Giménez, T. Cuadros, J. Bové, M. Martinez-Vicente, A. Parent, M. Gonzalez-Sepulveda, N. Peñuelas, A. Torra, B. Rodríguez-Galván, A. Ballabio, T. Hasegawa, A. Bortolozzi, E. Gelpi, M. Vila, *Nat. Commun.* 2019, 10(1), 973.

DOI:10.1038/s41467-019-08858-y

- 3. T.-S. Chang, *J. Mater.* **2012**, *5*(*9*), 1661–1685. **DOI:**10.3390/ma5091661
- T. Pillaiyar, V. Namasivayam, M. Manickam, S.-H. Jung, J. Med. Chem. 2018, 61(17), 7395–7418.
 DOI:10.1021/acs.jmedchem.7b00967
- F. Taranto, A. Pasqualone, G. Mangini, P. Tripodi, M. Miazzi,
 S. Pavan, C. Montemurro, *Int. J. Mol. Sci.* 2017, 18(2), 377.
 DOI:10.3390/ijms18020377
- 6. T. Pillaiyar, M. Manickam, V. Namasivayam, *J. Enzyme Inhib. Med. Chem.* **2017**, *32*(1), 403–425.

DOI:10.1080/14756366.2016.1256882

- B. Desmedt, P. Courselle, J. O. De Beer, V. Rogiers, M. Grosber, E. Deconinck, K. De Paepe, *J. Eur. Acad. Dermatol. Venereol.* 2016, 30(6), 943–950. DOI:10.1111/jdv.13595
- 8. Z. Peng, G. Wang, Y. He, J. J. Wang, Y. Zhao, *J. Curr. Res. Food Sci.* **2023**, *6*, 100421. **DOI:**10.1016/j.crfs.2022.100421
- A. Rescigno, F. Sollai, B. Pisu, A. Rinaldi, E. Sanjust, J. Enzyme Inhib. Med. Chem. 2002, 17(4), 207–218.
 DOI:10.1080/14756360210000010923
- Y.-M. Chen, W.-C. Su, C. Li, Y. Shi, Q.-X. Chen, J. Zheng, D.-L. Tang, S.-M. Chen, Q. Wang, *Int. J. Biol. Macromol.* 2019, 123, 723–731. DOI:10.1016/j.ijbiomac.2018.11.031
- J.-C. Cho, H. S. Rho, H. S. Baek, S. M. Ahn, B. Y. Woo, Y. D. Hong, J. W. Cheon, J. M. Heo, S.S. Shin, Y.-H. Park, K.-D. Suh, *Bioorg. Med. Chem. Lett.* 2012, 22(5), 2004–2007.
 DOI:10.1016/j.bmcl.2012.01.032
- 12. M. He, M. Fan, Z. Peng, G. Wang, Eur. J. Med. Chem. 2021, 221, 113546. DOI:10.1016/j.ejmech.2021.113546
- 13. Y.S. Lee, J.H. Park, M.H. Kim, S.H. Seo, H.J. Kim, *Arch. Pharm.* **2006**, *339*(3), 111–114. **DOI**:10.1002/ardp.200500213
- H. S. Rho, S. M. Ahn, D. S. Yoo, M. K. Kim, D.H. Cho, J. Y. Cho, *Bioorg. Med. Chem. Lett.* 2010, 20(22), 6569–6571.

- DOI:10.1016/j.bmcl.2010.09.042
- W. Yu, A.D. MacKerell, J. Antibiot. 2017, Vol. 1520, pp. 85– 106. DOI:10.1007/978-1-4939-6634-9_5
- R. Y. Choi, A. S. Coyner, J. Kalpathy-Cramer, M.F. Chiang, J. P. Campbell, *Transl. Vis. Sci. Technol.* 2020, 9(2), 14.
 DOI: 10.1167/tvst.9.2.14
- 17. S. Kolluri, J. Lin, R. Liu, Y. Zhang, W. Zhang, AAPS J. 2022, 24(1), 19. DOI:10.1208/s12248-021-00644-3
- M. R. Keyvanpour, M. B. Shirzad, Curr. Drug Discov. Technol. 2021, 18(1), 17–30.
 - DOI:10.2174/1570163817666200316104404
- M. D. Aytemir, B. Özçelik, G. Karakaya, *Bioorg. Med. Chem. Lett.* 2013, 23(12), 3646–3649.
 DOI:10.1016/j.bmcl.2013.03.098
- M. D. Aytemir, Ü. Çalış, *Arch. Pharm.* 2010, 343(3), 173–181.
 DOI:10.1002/ardp.200900236
- M. D. Aytemir, B. Özçelik, Eur. J. Med. Chem. 2010, 45(9), 4089–4095. DOI:10.1016/j.ejmech.2010.05.069
- G. Karakaya, A. Türe, A. Ercan, S. Öncül, M. D. Aytemir, Anticancer Agents Med. Chem. 2019, 18(15), 2137–2148.
 DOI:10.2174/1871520618666180402141714

- G. Karakaya, M.D. Aytemir, B. Özçelik, Ü. Çalış, *J. Enzyme Inhib. Med. Chem.*, 2013, 28(3), 627–638.
 DOI:10.3109/14756366.2012.666538
- G. Karakaya, A. Türe, A. Ercan, S. Öncül, M.D. Aytemir, *Bioorg. Chem.* 2019, 88, 102950.
 DOI:10.1016/j.bioorg.2019.102950
- 25. N. A. Frolov, A. N Vereshchagin, *Int. J. Mol. Sci.*, **2023**, *24*(3), 2937. **DOI:**10.3390/ijms24032937
- G. Karakaya, A. Türe, A. Ercan, S. Öncül, M. D. Aytemir, *Bioorg. Chem.* 2019, 88, 102950.
 DOI:10.1016/j.bioorg.2019.102950
- V. Vichai, K. Kirtikara, *Nat. Protoc.* 2006, 1(3), 1112–1116.
 DOI:10.1038/nprot.2006.179
- E. Frank, M. Hall, L. Trigg, G. Holmes, I.H. Witten, *J. Bioinform.* 2004, 20(15), 2479–2481.
 DOI:10.1093/bioinformatics/bth261
- 29. T.-S. Chang, *Int. J. Mol. Sci.* **2009**, *10*(6), 2440–2475. **DOI:**10.3390/ijms10062440
- 30. Q.-X. Chen, I. Kubo, *J. Agric. Food Chem*, **2002**, *50*(*14*), 4108–4112. **DOI:**10.1021/jf011378z

Povzetek

V tej študiji je bilo zgrajenih osem QSAR modelov za razvoj novih spojin kot inhibitorjev tirozinaze. Metode odločevalnih tabel, Bagging in Random comimittee so pokazale najboljše napovedne sposobnosti ($q^2 \ge 0.5$) med vsemi modeli. Na podlagi teh modelov je bilo sintetiziranih dvanajst novih derivatov kojične kisline. Inhibicija tirozinaze je bila določena s spektrofotometrično metodo z L-DOPA kot substratom. Za boljši vpogled v mehanizme inhibicije tirozinaze so bile izvedene študije molekulskega sidranja. Citotoksični učinki na celično linijo melanoma B16F10 so bili raziskani z uporabo SRB testa. Izveden je bil tudi test melanogeneze za zaznavo inhibicije tvorbe melanina. Spojine **4l**, **4j** in **4b** so pokazale boljši inhibitorni učinek na tirozinazo kot pozitivna kontrola, kojična kislina (218,8 μ M), z IC50 vrednostmi 138,1, 159,0 in 208,9 μ M. Spojina **4j** je izkazala najboljši protimelanogeni učinek med testiranimi spojinami. Ti izsledki potrjujejo potencial razvitih spojin kot novih inhibitorjev tirozinaze za klinične in kozmetične aplikacije.



Except when otherwise noted, articles in this journal are published under the terms and conditions of the Creative Commons Attribution 4.0 International License